

Supplementary Information for

**A simple angle-resolved thermal molecular beam reactor: applied to CO oxidation on Pt(110)**

Michael Bowker<sup>1,2,3</sup>, Björn U. Klink<sup>3,4</sup>, Kristian Lass<sup>3,5</sup> and Roger A. Bennett<sup>3</sup>

<sup>1</sup> Cardiff Catalysis Institute, School of Chemistry, Cardiff University, Cardiff CF10 3AT, UK

<sup>2</sup> Catalysis Hub, RCAH, Rutherford Appleton Laboratory, Harwell, Oxfordshire OX11 0FA, UK

<sup>3</sup> Department of Chemistry, University of Reading, Reading, RG6 6DX, UK

<sup>4</sup> Department of Structural Biochemistry, Max Planck Institute of Molecular Physiology, Otto-Hahn-Str. 11, 44227 Dortmund, Germany.

<sup>5</sup> Forensic Scientific Institute, State Criminal Police Office of Schleswig-Holstein, 24146 Kiel, Germany

### **1. Calibration of sticking experiments**

We noted in raw sticking measurement data a source pressure dependence on  $s_0$ . On investigation this was determined to be due to a difference in out of beam pressure rises measured in the chamber caused by a locally high pumping speed at the beam shutter. The pumping speed at the beam-defining aperture is considerably lower, leading to an additional background component. To calibrate the beam, we conducted sticking experiments with oxygen for different beam source pressures  $p$  and distances  $d$  between beam source capillary and skimmer cone. The results are shown in fig. S1.

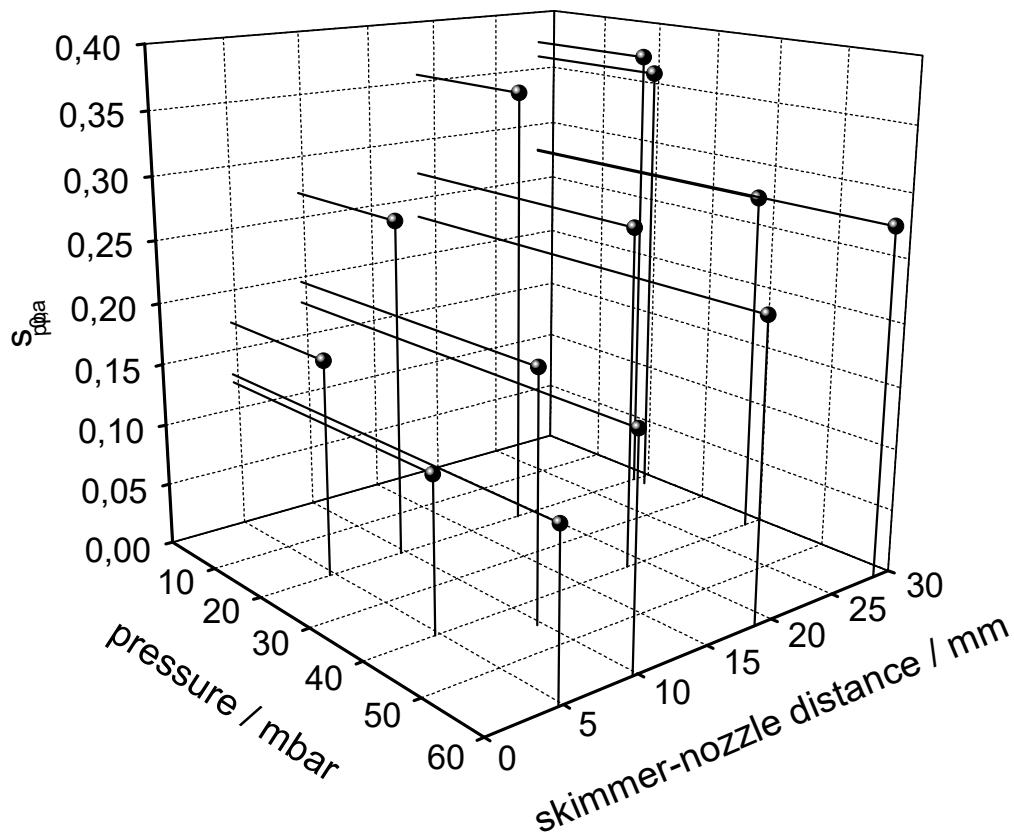


**Fig S1.** Apparent initial sticking probability  $S_{0,app}$  of oxygen at 420 K in dependency of beam source pressure and skimmer-nozzle distance.

The drop in apparent initial sticking probability with decreasing skimmer-nozzle distance and increasing beam source pressure indicates that both parameters influence the magnitude of the diffuse beam component. Reducing the source skimmer distance reduces the penumbra at the beam-defining aperture.

For a beam source pressure of  $p = 20$  mbar and a skimmer-nozzle distance of  $d = 29$  mm, the resulting initial sticking probability is consistent with the results of Walker et al. [1], indicating that the pressure rise is negligible under these conditions. Unfortunately, the signal-to-noise ratio is also quite low under these conditions because of the lower beam flux. While for oxygen this still gave a signal distinguishable from the background, the signal of CO was below the background level (CO is one of the major contaminants in the chamber). Because of this problem we decided to work with a higher beam pressure of  $p = 40$  mbar and a small skimmer-nozzle distance of  $d = 6$  mm and to calibrate our sticking probability values.

This was done by conducting cyclohexane sticking experiments. As reported by Jiang and Koel [2] cyclohexane has a sticking probability of unity in the temperature region 100 - 164 K. Calibration experiments with cyclohexane at 120 K gave an apparent sticking probability of  $s_{app} = 0.45 \pm 0.01$  for the normal beam setup of  $p = 40$  mbar and  $d = 6$  mm. The sticking probability values for other gases were calibrated by this value.

## 2. Scattering

The scattering profile for He, Ar and O<sub>2</sub> from Pd(111) is shown in in fig. S2 which shows a clear specular reflection for all three elements at 67.5°. In comparison to Pt{110}(1×2) all elements are sharper when scattered directly from the Pd(111) surface due to the collimated beam and direct scattering events.

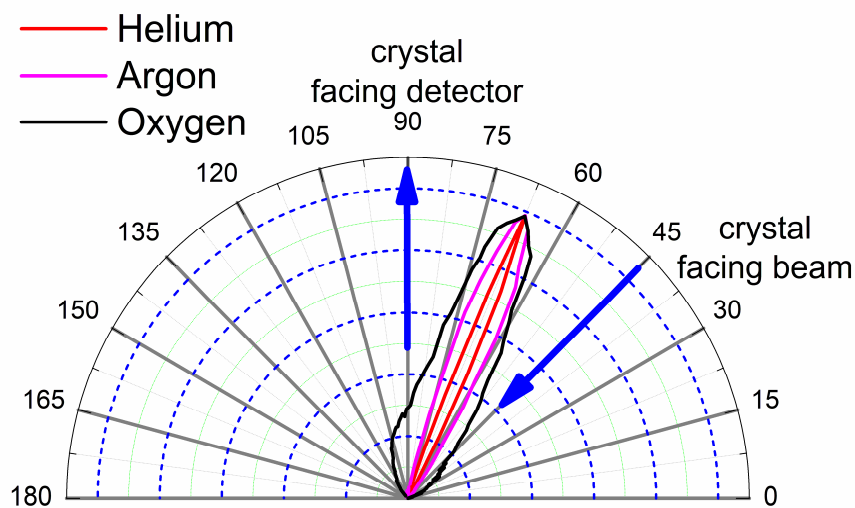


**Figure S2** He, Ar and O<sub>2</sub> scattering from Pd(111) at 373 K, 573 K and 873 K respectively, to avoid trapping – desorption influencing the angular profile. O<sub>2</sub> scattering in particular has a large trapping component and relatively small specular component below 673K. The extremely sharp He reflectivity can be fit with a  $\text{Cos}^\alpha$  profile with  $\alpha = 600 \pm 15$  exponent which indicates the system angular resolution.

The scattering on the surface is not fully elastic which causes a broader distribution of the gas atoms due to partial accommodation on the surface. As this effect increases with increasing mass of the scattered atoms and lower temperature, it largely contributes to the observed broad scattering of the Argon atoms from Pt. Furthermore, the Pt{110}(1×2)

surface does not show an ideal missing-row structure, exhibiting a ‘fish-scale’ pattern, as reported by Speller et al. [3] from STM investigations. This may give rise to a broad scattering of bigger atoms like argon, causing the coalescence of the two peaks in this case. The argon atoms feel a less corrugated surface potential, resulting in a narrowing of the gap between the two peaks. This effect may also be responsible for the small difference between the scattering angles for helium found in experiment and simulation. Taking all these effects together, they are sufficient to explain the broad Argon scattering result.

### 3. Oxygen Sticking.

Some examples of our sticking curves as a function of oxygen uptake at different temperatures are shown in the supplementary information, and figs fig. 1.

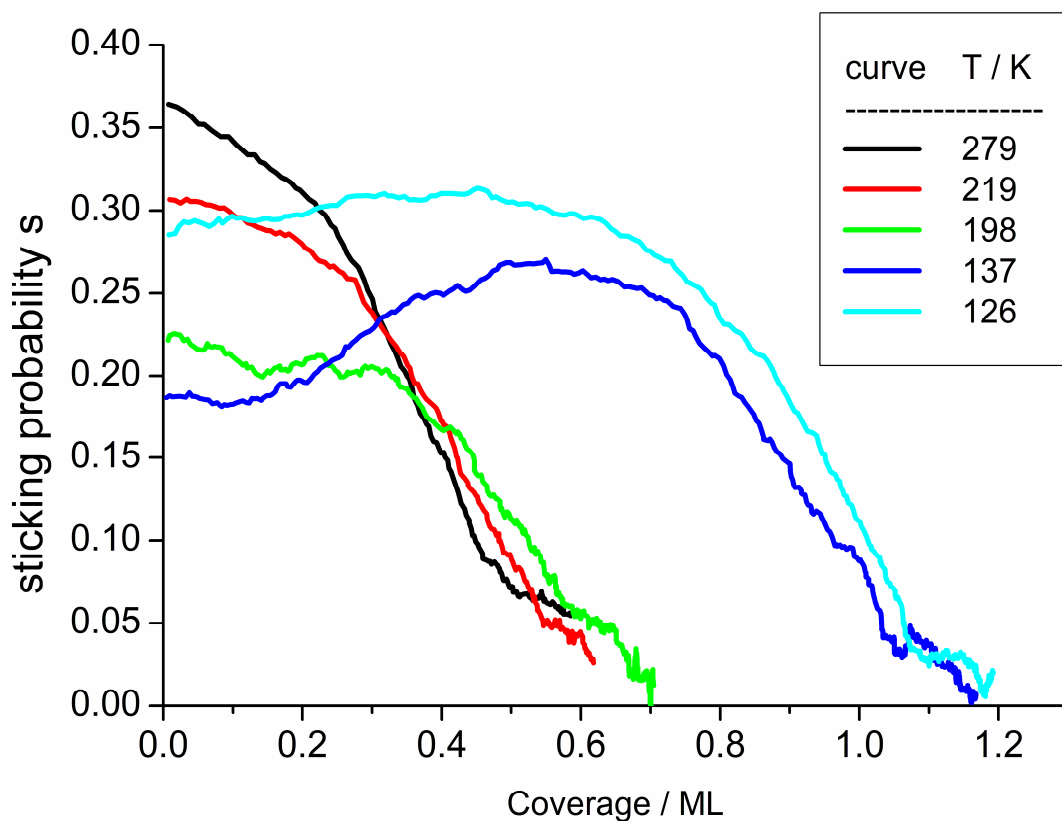
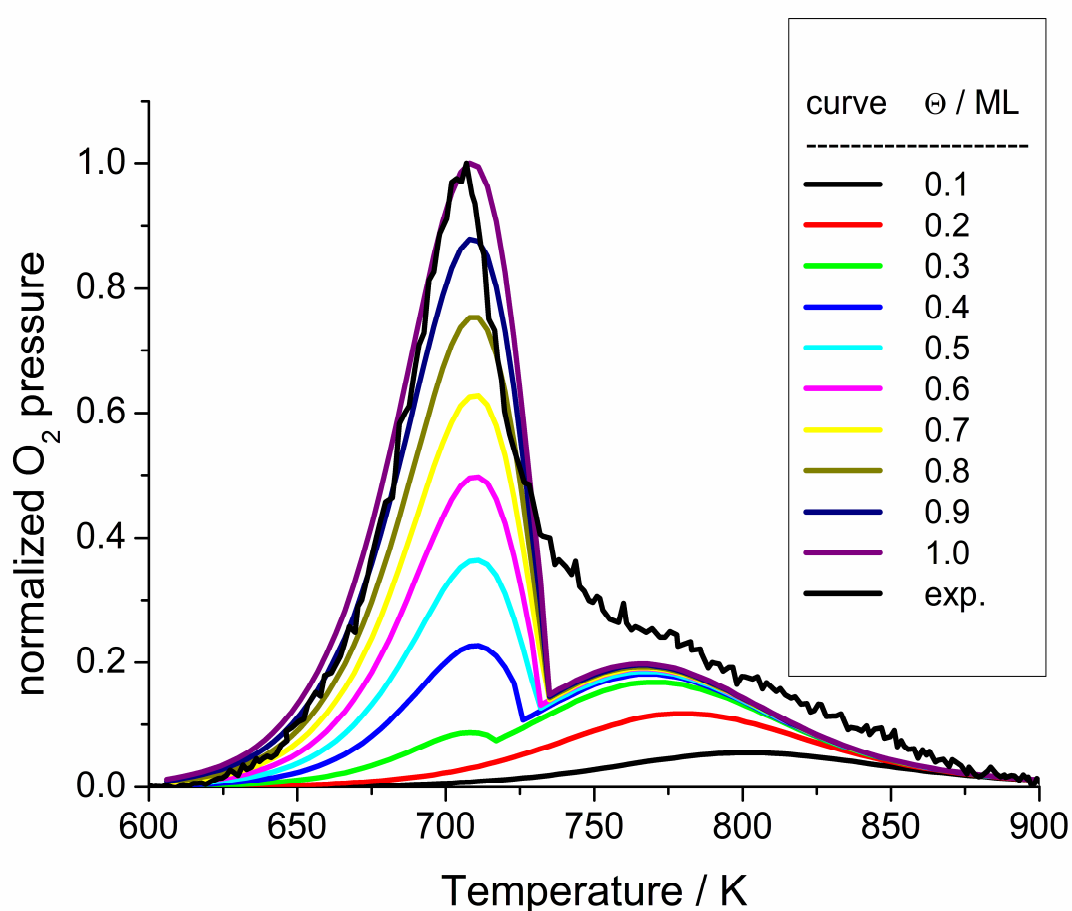


Fig S3. Sticking probability of oxygen as a function of uptake for different sample temperatures.

An increase in sticking probability is evident at temperatures lower than 200K. An incoming O<sub>2</sub> molecule may collide with a pre-adsorbed O<sub>2c</sub> species and due to enhanced mass matching yield a higher trapping probability. This results in an increase in the sticking probability *s* at low coverages of oxygen as observed by Walker et al. [1]. From the increase of the sticking probability with increasing coverage, Walker et al. estimated the coverage of O<sub>2c</sub> islands to be about 1/3 ML.

#### 4. TPD Curve fitting



**Fig S4.** Simulated oxygen TPD spectra. The preexponential factor  $\nu$  and the desorption activation energy  $E_d$  have been varied as indicated in the figure.

The best agreement with the shape of our curves regarding the peak maximum temperature and the peak widths of the curves could be obtained using a frequency factor of  $1 \times 10^{16} \text{ s}^{-1}$  and a desorption energy of 230 kJ/mol for the  $\beta_1$  state. For the  $\beta_2$  component of simulation

with  $\nu = 1 \times 10^{10} \text{ s}^{-1}$  and  $E_d = 155 \text{ kJ/mol}$  gave optimal shapes even though higher than literature values.

### 5. Angle-resolved product distributions

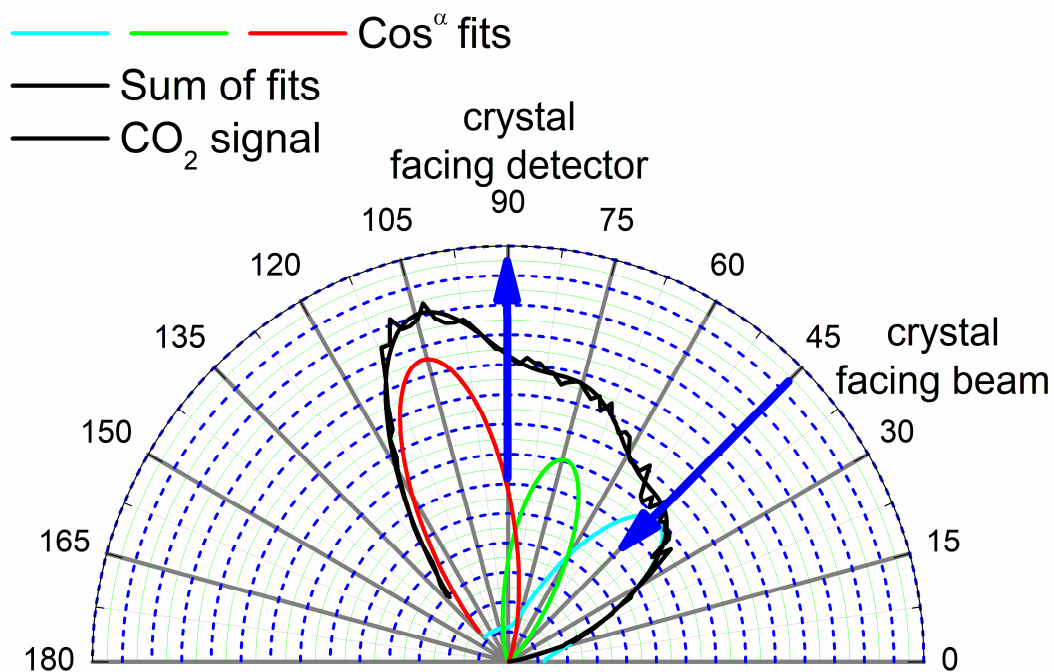


Fig S5a. Angle-resolved CO oxidation experiment as in fig 13, at 523 K surface temperature.

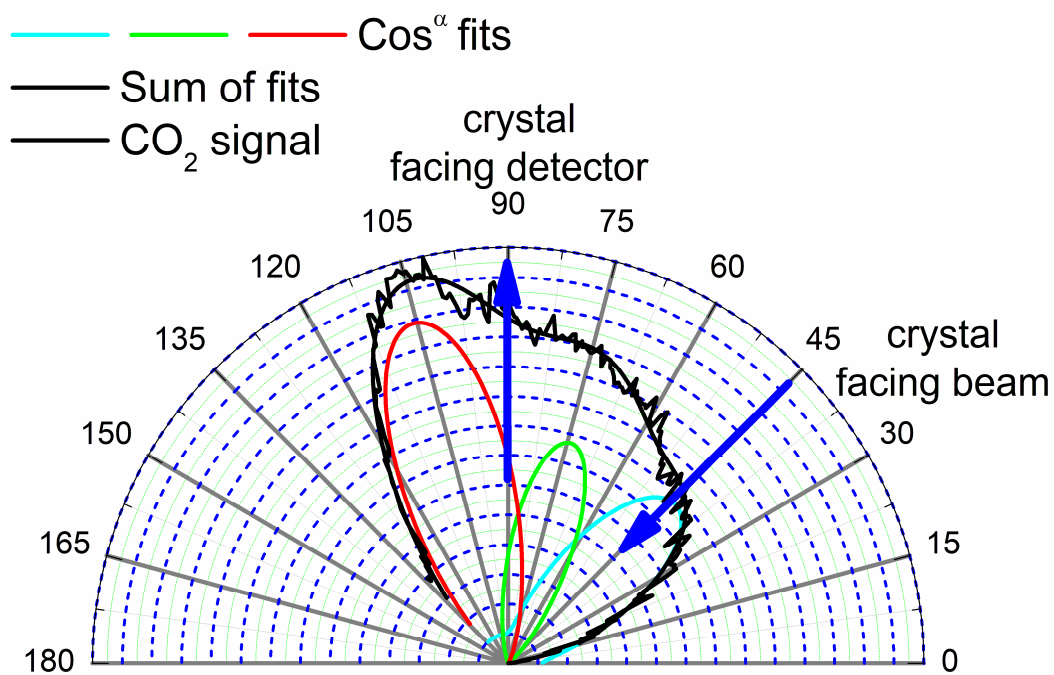


Fig S5b. Angle-resolved CO oxidation experiment as in fig. 13, at 573 K surface temperature

1. Walker, A.V., B. Klötzer, and D.A. King, *Dynamics and kinetics of oxygen dissociative adsorption on Pt{110}(1×2)*. The Journal of Chemical Physics, 1998. **109**(16): p. 6879-6888.
2. Jiang, L.Q. and B.E. Koel, *Hydrocarbon trapping and condensation on platinum (111)*. The Journal of Physical Chemistry, 1992. **96**(22): p. 8694-8697.
3. Speller, S., et al., *The (1 × 2) and (1 × 4) structure on clean Pt(110) studied by STM, AES and LEED*. Surface Science, 1996. **366**(2): p. 251-259.